ELSEVIER

Journal of Nuclear Materials 257 (1998) 152–161

journal of nuclear materials

A study on the reaction of yttria (Y_2O_3) in flowing uranium hexafluoride (UF_6) gas at 900°C

Ziya Engin Erkmen *

Department of Metallurgy and Materials, Istanbul University, Avcilar Campus, 34850 Avcilar – Istanbul, Turkey

Received 20 January 1998; accepted 14 May 1998

Abstract

The corrosion behaviour of Y_2O_3 (yttria) at 900°C in flowing UF_6 (uranium hexafluoride) was investigated under a pressure of 1.33×10^{-3} Pa. A test loop was used to study the chemical reaction of sintered and hot-pressed yttria samples with flowing UF_6 gas in an alumina reaction tube installed in an electrically heated horizontal 1200°C type furnace. A weight increase was observed after each exposure testing. Scanning electron microscopy (SEM) examination of the exposed samples identified two layers of reaction products. Significant cracking and porosity were observed in the outer layer after the experiment while the inner layer thickness decreased with increasing the exposure time. Thermodynamical analysis using Facility for the Analysis of Chemical Thermodynamics (FACT) software packages has been performed and relevant interface reactions have been suggested. Pilling–Bedworth Ratios for both layers were calculated and found to be in agreement with the morphology of the layers. Electron microprobe (EMP) and X-ray diffraction analysis (XRD) revealed the formation of UO_2 and YF_3 in the outer layer and a possible formation of YOF in the inner layer. The formation of the outer layer was primarily due to oxygen–fluorine exchange reactions between yttria and uranium fluorides while the inner layer was a direct consequence of the fluorine inward diffusion and reaction with yttria.

1. Introduction

Gas core nuclear reactors fuelled by uranium fluoride gases (UF_n, $n = 4$, 6) are considered for a variety of space, power and propulsion applications. The highly corrosive nature of UF_6 and UF_4 at elevated temperatures (700–3700°C) and the high neutron fluxes constitute a major material problem for the inner walls and the nozzle portion of gas core reactors and magnetohydrodynamic (MHD) system. In order to overcome the destructive effects of the gas at high temperatures, special materials have to be developed which possess high melting points, low neutron absorption cross-sections and high stability (large negative Gibbs energy of formation). If any reaction occurs, it is desirable that a protective layer forms on the surface, which can stop the corrosion from extending further through the material.

Yttria (Y_2O_3) is a high melting point ($T_{melt} = 2410$°C), very stable oxide ceramic with relatively low thermal neutron absorption cross-section (1.4 barns). Fig. 1 compares the free energy of formation for yttria, alumina (Al_2O_3), beryllia (BeO), thoria (ThO_2) and zirconia (ZrO_2). The higher negative free energy of yttria combined with the high melting point of yttrium fluoride (YF_3, 1387°C) suggest the compatibility of this ceramic with a fluorine rich environment. Holcombe et al. [1] conducted the exposure testing of yttria and several other oxide ceramics to a mixture of hydrogen and fluorine flame ($1H_2/2F_2$) at temperatures above 800°C. Formation of a protective layer of yttrium fluoride on yttria samples was reported below the failing point of the YF_3 film at 1147°C. The corrosion rate of other oxide ceramics in fluorine rich environments was also attributed to the failing point of their metal fluoride films. Whitney et al. [2] tested yttria, alumina, magnesia, pyrophyllite which were exposed to stagnant uranium hexafluoride (UF_6) at 700°C and 11.60 kPa pressure for 1 h. None of the exposed ceramics showed any sign of

* Tel.: 90-212 591 1998; fax: +90-212 591 1997; e-mail: eerkmen@mail.istanbul.edu.tr.

0022-3115/98/$ – see front matter
PII: S0022-3115(98)00437-1

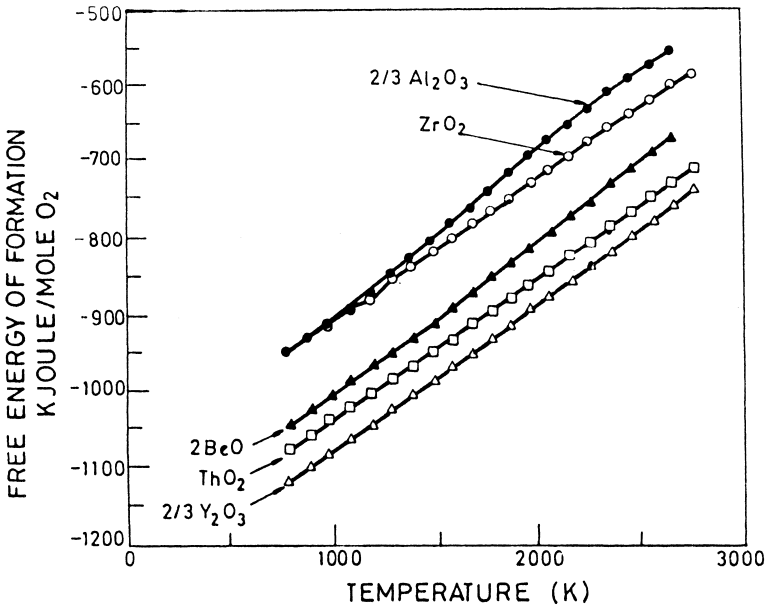

Fig. 1. Comparison of the free energy of formation for yttria and several other highly stable oxides (after Anderson, 1971).

corrosion by UF_6 gas below 700°C. Collins [3] reported another UF_6 corrosion study involving ZrO_2 in which UF_6 reacted completely with zirconia at 800°C, forming uranium oxides, zirconium fluorides and zirconium oxyfluorides. A more recent study of UF_6 reaction with alumina ($A1_2O_3$) at higher temperatures was conducted by Wang et al. [4]. Sapphire and polycrystal alpha alumina were tested and the maximum service temperature of alumina was found to be 1000°C.

This paper presents the results of yttria reaction with UF_6 and its possible reaction mechanism at high temperatures.

2. Experimental procedure

Sample preparation: The yttria powder used in this experiment was approximately 1 μm in average size and 98% purity (Morton Thiokol, Alfa Products, Danvers, MA). In order to increase the density, sintering and hot pressing were performed to obtain disk shape samples from powder.

Sintering: Yttria powder was cold isostatically pressed to 170 MPa pressure for 10–15 min. The diameter and thickness of the processed yttria disks were 2.54 and 0.20 cm, respectively. The green yttria disks were then mounted on a mullite plate for sintering. Yttria powder was added between the plate and the disks to prevent contamination of the sample by the mullite substrate. Samples were heated in an electric furnace (Deltec Model 31-DTS-1, Deltec, Denver, CO) to a maximum of 1700°C at a rate of 200°C/h under ambient atmosphere. Then, they were kept for 1 h at 1700°C and subsequently cooled to room temperature over a period of 25 h [5–7]. Archimedes' method was used to measure the density of the samples according to ASTM C 20-80a standards [8]. Nearly 85% theoretical density samples were obtained using the sintering process. For convenience, samples obtained through this process are called Ytt85.

Hot pressing: A graphite die having a compression strength of 117 MPa was used to form high-density yttria disks in the hot-press. The inner wall of the die was coated with boron nitride (BN) to prevent yttria from being in contact with graphite. After placing the die containing the green disk in the hot-press, the temperature was slowly increased by inductive heating to about 500°C at a rate of 5–6°C/min under argon atmosphere. The sample was held at this temperature for 1 h. Next the temperature was raised to 1600°C and a pressure of 30 MPa was applied. Same procedure was repeated for a second sample, this time at 1700°C and 45 MPa pressure. The samples were kept at these pressure and temperature ranges for 1.5 h. Finally, the furnace was turned off and samples were left to cool down in the furnace. At the end of the process, the colour of the samples had turned from white to black. This was probably due to carbon diffusion into the sample under high pressure and temperature. Referring to thermodynamics [9,10] at 900°C, there was no reaction occurring between carbon and yttria in carbon doped yttria. Both components kept their stability at the experimental conditions ($C + Y_2O_3 \rightarrow C + Y_2O_3$). Consequently, a heat treatment on the samples was performed: yttria disks were placed in an electric furnace and heated to a

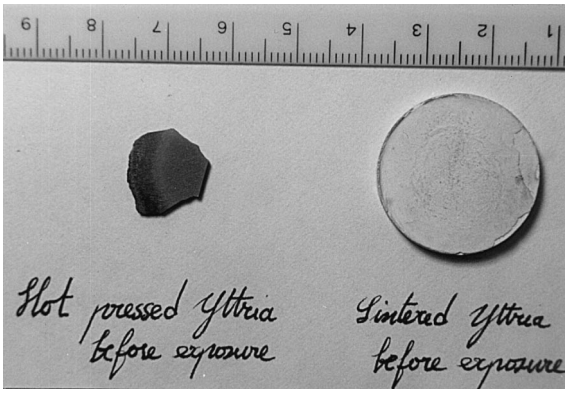

Fig. 2. View of a broken piece of hot-pressed and sintered sample.

maximum of 1200°C in air for 3 h. Following this procedure, the colour of yttria samples changed from black to white as the carbon was oxidized. The Gibbs free energies of formation were calculated to be $\Delta G(Y_2O_3) = -10474$ kJ and $\Delta G(CO) = -10244$ kJ for 900°C and 0.365 atm pressure. Since the former is thermodynamically more stable than the latter, there was no oxygen lost by yttria during the heat treatment which otherwise would have made it non-stoichiometric. Samples with densities higher than 99% of theoretical density were called ytt99.

Finally, samples were cut with a diamond saw and prepared for testing. Fig. 2 shows a broken piece of the hot pressed material (very brittle when removed from the die) and a whole piece of a sintered sample.

Exposure of yttria to UF_6: The corrosion test of yttria by UF_6 gas was carried out in a flowing loop test unit. A schematic diagram of the unit is shown in Fig. 3. Uranium hexafluoride which is a by-product of the uranium enrichment process was supplied by the Oak Ridge National Laboratory. The reaction chamber was made of 98% pure alumina tube 61-cm long and 1.27-cm inner diameter. $A1_2O_3$ was chosen for its relative compatibility with UF_6 at elevated temperatures. The reaction chamber was connected to the loop by inserting Monel tubes for about 2.5 cm into each end of the alumina tube. They were then bonded together from the outside using a high temperature ceramic adhesive. A coating of Torr-Seal epoxy was applied to the outside of these joints to provide a vacuum-tight seal. Two Monel cylinders were installed in the system, one for UF_6 supply and the other as a cold trap. The second cylinder was cooled in a liquid-nitrogen Dewar, thereby providing a passive driving force for flowing the UF_6 through the system and also removing any condensable reaction products. Uranium hexafluoride with a purity of 99.99% and with a depletion level of less than 0.3% of uranium-235 was supplied in solid–vapor form. Based on the energy balance and differential pressure measurement, the UF_6 throughput during the experiment was estimated to be on the order of 5 g/s. After the weight and the surface area of the samples were measured, they were laid on an alumina boat and inserted in the alumina reaction tube which was placed then at the center of a 1200°C horizontal furnace. The test system was evacuated to a 10^{-3} Pa (10^{-5} Torr) using a diffusion pump. Monel tubing and joints were wrapped with heating tapes and heated to about 145°C to keep UF_6 in the gas phase so that a quasi-steady flow of UF_6 was through the test chamber. The furnace temperature was increased to 900°C at a rate of 150°C/h before releasing UF_6. During the experiment, two pressure transducers were

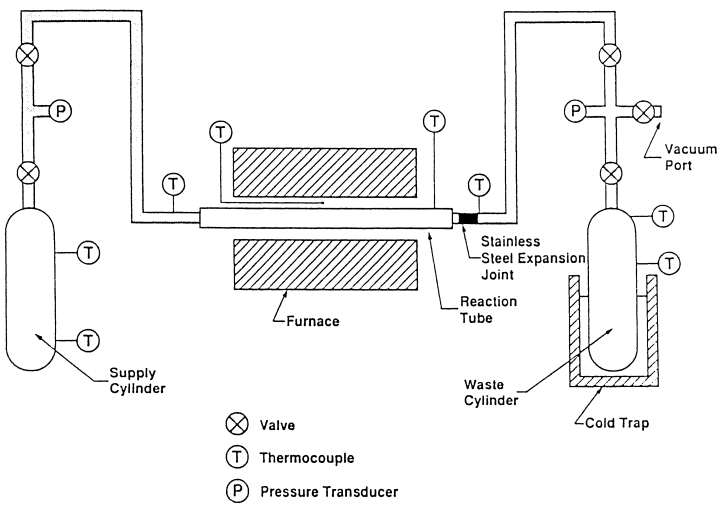

Fig. 3. Schematic diagram of the flowing UF_6 test system.

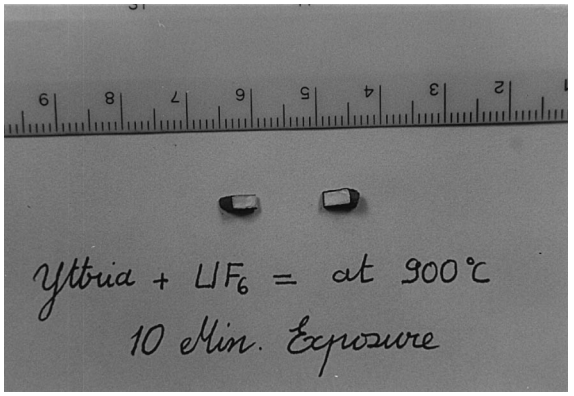

Fig. 4. Reaction product layers of yttria samples after UF_6 exposure.

used to monitor gas flow through the system. Typical pressures measured during the test were 3.76×10^4 Pa (282 Torr), 3.65×10^4 Pa (274 Torr) for reaction tube inlet and outlet, respectively. After completion of the exposure test and system cool-down, the alumina reaction tube was removed and the samples were taken out. Residual weights of the exposed samples were measured using an ultra-high-precision electronic balance.

Preliminary exposure of yttria was done at 800°C for 90 min. At the end of the exposure, no visible reaction was observed on the surface of the yttria sample. However, a test conducted for 90 min at 900°C resulted in complete decomposition to the point that no solid piece was left in the reaction chamber. Hence, in order to study the reaction of yttria with UF_6 at 900°C, the exposure time was reduced to a maximum of 25 min. In Fig. 4, reaction products on the samples can be seen as a black layer surrounding the white yttria substrate.

3. Post-test analysis

Weight change analysis: The weight of the samples was measured before and after the test using a digital microbalance with an accuracy of 5 decimal points. This was a discontinuous process for different exposure times due to the highly corrosive nature of the experiment which prevented us from using TG instrument. In general, a weight increase was observed for Ytt85 and Ytt99 samples after exposure at 900°C. Results are shown in Table 1. For exposure times less than 15 min, samples maintained their shape and a relatively thin black layer of reaction products formed on their surfaces. After exposure for 20–25 min, both Ytt85 and Ytt99 samples were found to be cracked and decomposed. Reaction products formed a low-density porous layer with an irregular shape on the surface of the samples.

Table 1
Weight change results of yttria reacting with UF_6 at 900°C

Sample	Test time (min)	Weight change (%)
Ytt85	5	25.5
Ytt85	10	6.9
Ytt85	15	9.3
Ytt85	20	29.2
Ytt85	25	31.8
Ytt99	20	47.6
Ytt99	25	47.2

SEM/EMP analysis: For scanning electron microscopy (SEM) analysis, the reacted Ytt85 samples were cut, and the cross-section area was polished down to 1 μm using diamond powder. Samples were then coated with a thin layer of carbon for the analysis. Basically, two layers of reaction products were observed under the SEM on the sample surface tested in UF_6 at 900°C for 5, 10, 15, 20 min. The external porous layer (outer layer) and the internal layer (inner layer) are shown in Fig. 5.

Electron microprobe (EMP) analysis was performed to study the elemental concentration profiles in these reaction zones. Results of post-test analysis of Ytt85 samples after exposure for 5, 10 and 20 min are given in Figs. 6–8, respectively. Figs. 6(a),7(a) and 8(a) show the micrographs of the polished cross-sectional area of the samples where the EMP analyses were conducted. This was performed by scanning the sample for a total of 100 μm. The relative concentration profiles for reacting elements are plotted with reference to their micrographs in Figs. 6(b), 7(b) and 8(b).

The elemental analysis by EMP established the formation of two layers of reaction products with different chemical constituents. The outer layer consisted of yttrium, fluorine and uranium atoms where the inner layer included yttrium and fluorine atoms. It should be noted that due to the limitation in calibration, the oxygen

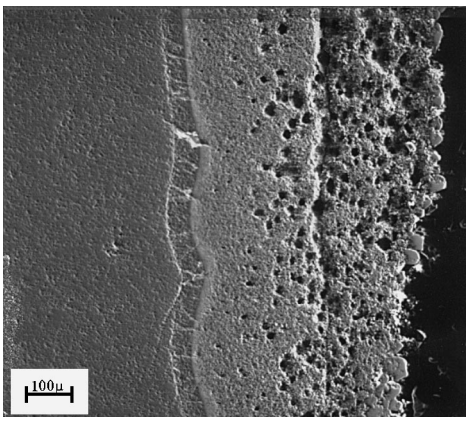

Fig. 5. Cross-section micrograph of Ytt85 sample after exposure to UF_6 at 900°C for 10 min.

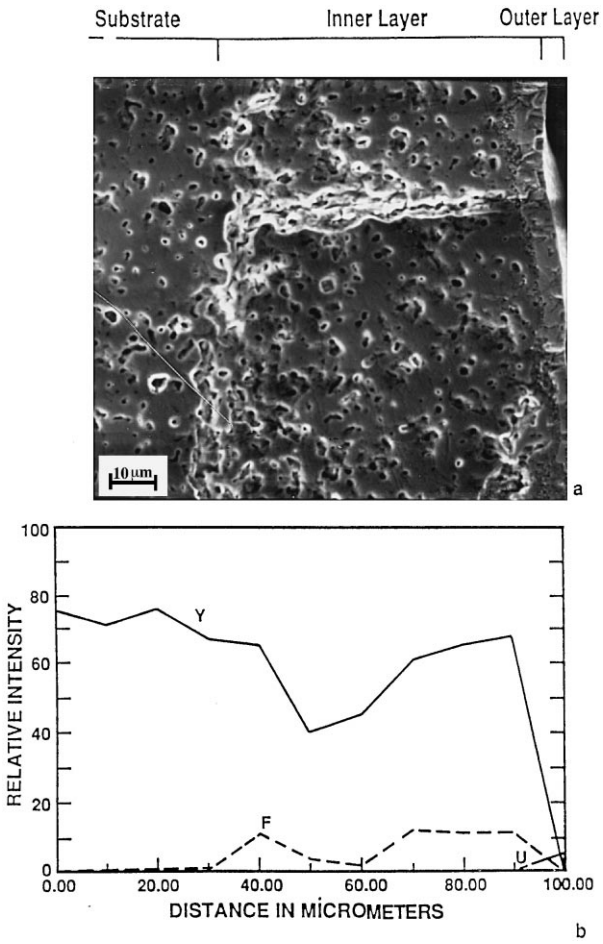

Fig. 6. Result of EMP analysis for ytt85 sample after exposure to UF_6 at 900°C for 5 min. (a) Micrograph of the exposed sample cross-section. (b) Elemental concentration profiles.

atom was not detected by EMP. The thickness of the inner layer was determined to lie between the end points of uranium concentration at the outer interface (the interface of the inner and outer layer) and fluorine concentration at the inner interface (the interface of substrate and the inner layer). It was found that the thickness of the inner layer decreased from 90 to 55 μm as exposure time increased from 5 to 20 min (Figs. 6–8).

XRD analysis: X-ray analysis which was performed on the ground samples, identified YF_3, UO_2, UO_3, YOF as the reaction products. Similar X-ray diffraction analysis (XRD) results were obtained for different exposure times. In Fig. 9, a typical diffraction pattern for a 20-min exposure is presented. The standard patterns of the identified components (YF_3,UO_3 and YOF) taken from JCPDS reference cards are also shown in Fig. 9 for comparison with the sample pattern. The intensities between the experimental pattern and the standard patterns were not exactly matched due to the overlapping of different compounds.

Thermodynamic analysis: The prediction of possible chemical reactions and end products at specific combinations of temperature and pressure was performed using the Facility for the Analysis of Chemical Thermodynamics (FACT) computer database and computer code package [10]. In this package, the equilibrium program (EQUILIBR) was used to analyse the reactions of UF_6, UF_4, and F_2 with yttria at 900°C and 0.365 atm (278 Torr) pressure. This program determines the molar concentrations of product species when specified elements or compounds react to reach chemical equilibrium. The calculation of the equilibrium concentration is based on the minimisation of the total free energy of the system.

4. Discussion

In this work, the results of yttria (Y_2O_3) exposure to UF_6 at 900°C and 37 KPa (278 Torr) showed a different

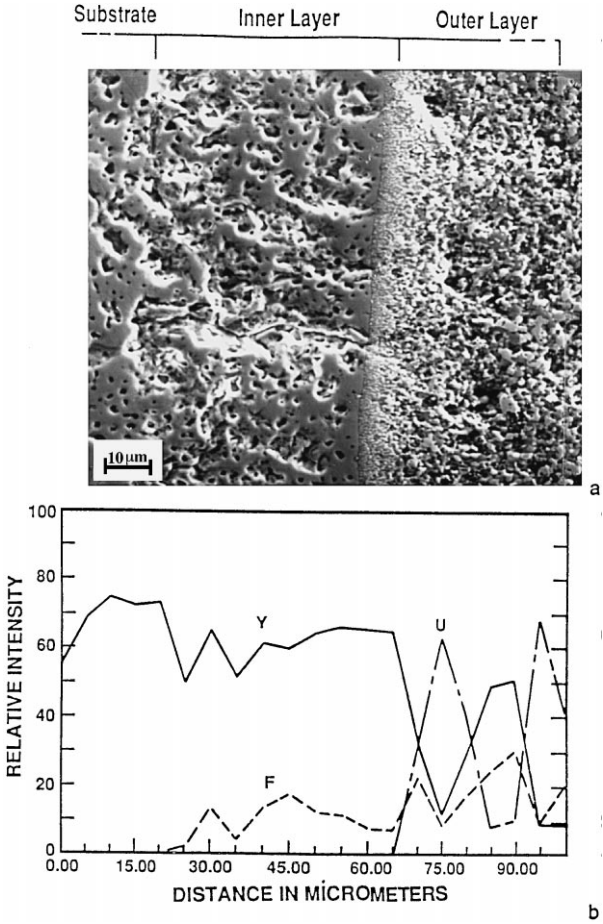

Fig. 7. Result of EMP analysis for ytt85 sample after exposure to UF_6 at 900°C for 10 min. (a) Micrograph of the exposed sample cross-section. (b) Elemental concentration profiles.

trend than the results obtained by Holcombe et al. [1] and Whitney et al. [2]. Formation of a protective YF_3 layer was not observed in our experiments, contrary to what was reported by Holcombe et al. who noted a high fluoride film failure temperature (1150°C) in their exposure of yttria to a H_2/F_2 flame. For the fluoride layer to be of a protective nature, certain criteria must be considered, these can be summarized as follows: the scale should have good adherence, a high melting point and low vapour pressure to resist evaporation. In addition, the fluoride film and substrate should have nearly the same thermal expansion coefficients to accommodate differences in their specific volumes and thermal expansions. The properties of relatively thin films are difficult to measure or predict in situ. Therefore, only a qualitative treatment of the scales has been given in this study.

The dissociation of UF_6 to form F_2 and other lower uranium fluoride compounds at temperatures above 700°C [2] suggested that the extensive corrosion was due to the reaction of a mixture of UF_6 and its dissociation products. The sharp weight increase at 20 and 25 min exposure time and the complete decomposition of the sample for testing times more than 1 h indicated that the film failure temperature of YF_3 in UF_6 gas was below 1150°C for the experimental conditions. The presence of uranium, yttrium and fluorine detected by EMP in the outer layer suggest that the outer layer was mainly composed of UO_2 and YF_3 in accordance with the XRD results and the intact substrate remains Y_2O_3.

The product phases obtained after the experiments agree with the thermodynamic calculation [10] given as reactions I, II and III. The melting temperatures of YF_3 and UO_2 are 1387°C and 2878°C, respectively which were well above the test temperature.

I. $3UF_4 + 2Y_2O_3 \rightarrow 4YF_3 + 3UO_2$,
ΔG (900°C) = −117 kcal/mol,
II. $3UF_6 + 3Y_2O_3 \rightarrow 6YF_3 + U_3O_8 + \frac{1}{2}O_2$,
ΔG (900°C) = −308 kcal/mol,
III $3F_2 + Y_2O_3 \rightarrow 2YF_3 + \frac{3}{2}O_2$,
ΔG (900°C) = −308 kcal/mol.

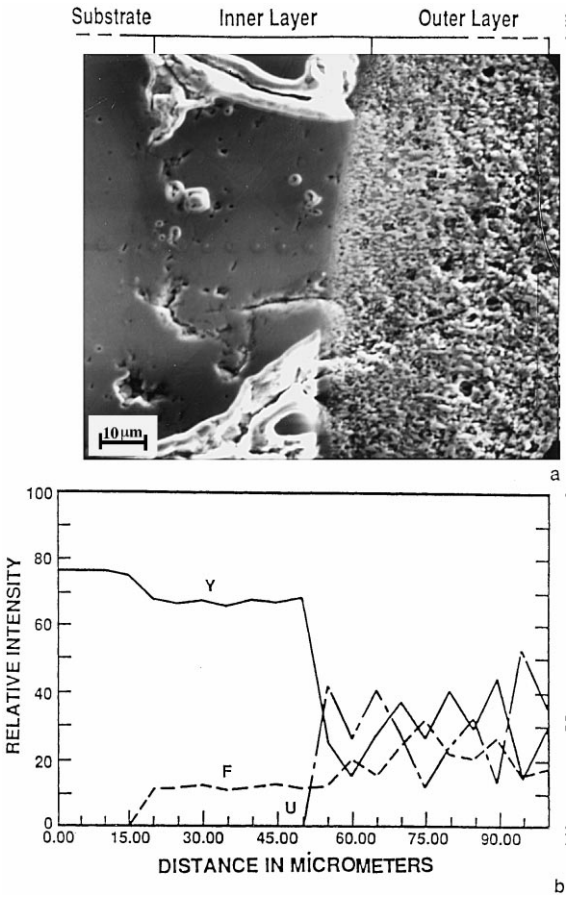

Fig. 8. Result of EMP analysis for ytt85 sample after exposure to UF_6 at 900°C for 20 mm. (a) Micrograph of the exposed sample cross-section. (b) Elemental concentration profiles.

As observed by earlier researchers [3,11,12], UO_2F_2 did not appear in the X-ray patterns most probably due to the decomposition of $UO_2F_{2(s)}$ to U_3O_8, UO_2, UF_6 and UF_4 above 700°C. Similarly, an intermediate compound YOF (thermodynamic data for which does not exist in the FACT software package, JCPDS card no: 38-746) is probably formed during the reactions and may form the inner layer. A recent study [13] carried out on aluminium corrosion by UF_6 showed that the formation of uranium oxyfluoride (UO_xF_y) occurred on the surface of the corroded samples from 20°C to 200°C which strengthens the above statement. The UOF compound was not detected by XRD, because it was probably hidden in the background due to the very thin nature of the inner layer. Based on the arguments given above, the interface reactions can be suggested as follows.

Along the interface of substrate–inner layer

IV. $F_2(g) + Y_2O_3(s) \rightarrow 2YOF(s) + \frac{1}{2}O_2$ (g).

Along the interface of outer–inner layer

V. $3YOF + UF_6 \rightarrow UO_2 + 3YF_3 + \frac{1}{2}O_2$.

VI. $2YOF + UF_4 \rightarrow UO_2 + 2YF_3$.

At the first contact of UF_6, and its dissociated products F_2, UF_4 with yttria, the inner layer is formed according to reaction IV by the rapid diffusion of fluorine through the substrate. The small size of fluorine molecules with respect to UF_6 and UF_4 ($r_F = 0.64$ Å, $r_U = 1.05$ Å) [14] and its probable higher diffusion rate in YOF caused the formation of an approximately 60 μm thick inner layer during the first 5 min (Fig. 6). After 10 min of exposure testing a substantial amount of a secondary layer has been formed (Fig. 7). In the meantime, the diffusion of fluorine molecules was retarded as the outer layer grew inward by corroding the inner layer according to reactions V and VI. As the secondary scale grew, it produced stresses which resulted in cracking and spallation, allowing gaseous species to reach the inner–outer layer interface more rapidly. After cracking and spallation occurred, the porous structure of the outer layer allowed for the high rate of gas transfer which accelerated the corrosion of the inner layer. This layer has shrunk to 35 μm after 20 min exposure testing (Fig. 8). An illustration of layer formation is given in Fig. 10(a).

Due to the limited amount of information available in the literature, a physical qualitative description of the electronic phenomena involved in these processes can only be drawn by simulating the well-known models of the scaling of iron (FeO, Fe_3O_4, Fe_2O_3), cobalt (CoO, Co_3O_4), titanium (Ti_2O_3, TiO) and copper (Cu_2O, CuO) accompanied by the multiscale layers formation [15–18] during their high temperature oxidation.

To simulate the oxidation model, some assumptions should be made for our case. The shrinkage of the inner layer suggests that the outer scale grows at the inner–outer scale interface rather than the scale–gas interface. This can happen by anion migration. In order to explain simultaneous migration of ions and electrons, it is necessary to assume that the fluorides, oxides that are formed during the reaction are non-stoichiometric compounds [15].

In addition

1. The substrate Y_2O_3 and inner layer YOF are n-type anion deficient semiconductors in which the electrical charge is transferred by negative carriers according to $O_o = V_o + 2e^- + \frac{1}{2}O_2$. O_o: Oxygen in oxygen site, V_o: oxygen vacancy with two positive charges.

2. The inner fluoride-layer is a compact, perfectly adherent scale.

3. Thermodynamic equilibrium is established locally throughout the inner scale and at both the substrate–inner layer and inner layer–outer layer interface.

During the corrosion reaction, as mentioned earlier, the fluorine anions will migrate through Y_2O_3, substituting oxygen vacancies and forming a YOF layer which will

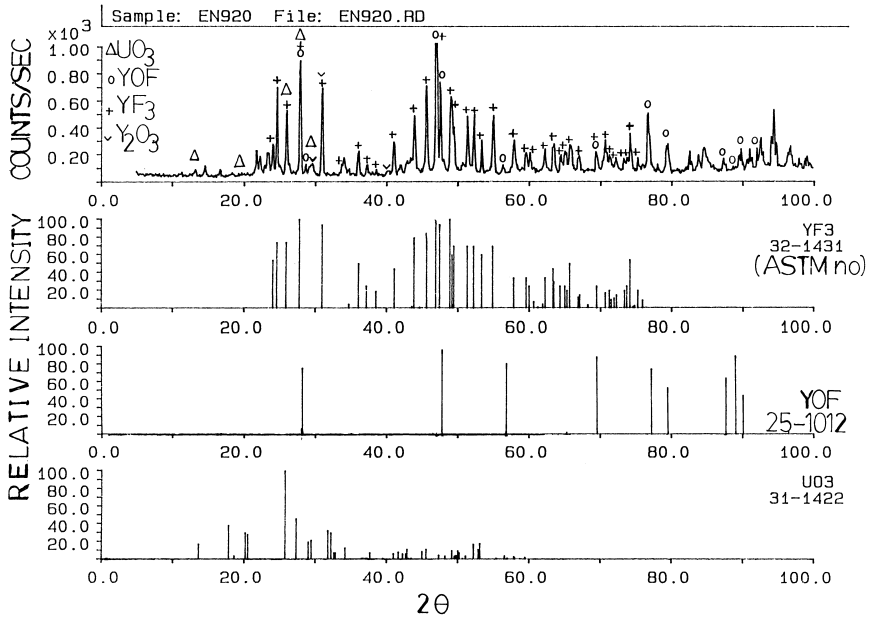

Fig. 9. X-ray diffraction pattern of Ytt85 reacted with UF_6 at 900°C for 20 min and reference patterns of the YF_3, YOF, UO_3 compounds.

grow inwardly. In the meantime, to hold the electrical neutrality, there would be a counterflow of anion vacancies and electrons towards the gas oxide interface. At some later stage, an outer layer is formed by the consumption of the inner layer according to reactions V and VI as observed experimentally from Figs. 6(b), 7(b), and 8(b). The diminishing inner layer weakens the argument of outward diffusion of metal cations via cation vacancies and strengthens the assumption that Y_2O_3 and YOF were n-type non-metal deficient oxides, or otherwise the scale would grow outwardly with the diffusion of positively charged Y^{+++} cations (such in the oxidation of iron where the growing scales FeO, Fe_3O_4, Fe_2O_3 are p-type metal deficient semiconductors and the diffusion of cations controls the overall reaction rate). A physical scheme of the electronic exchange is given in Fig. 10(b) and (c).

The physical nature of both layers are different: the porous spongy outer scale, after 20 min exposure cracked, flaked and spalled. The solid products after reaction I and reaction II were used to estimate the scale densities and weights. The Pilling–Bedworth ratios [1] of the outer and inner layer were calculated to be nearly 0.65 and 1.20, respectively. The former is less than one showing the scale is not necessarily coherent. This is consistent with its porous character assuming that PB treatment would also be valid for fluoride films. The inner layer is however coherent allowing the oxygen and fluorine ionic diffusion to progress through the layer. The UO_2 component alone has a PB ratio of 1.97 and forms a non-protective scale [19].

In order to derive a complete model of this diffusing and simultaneously reacting system which essentially possesses 4 components and 4 phases, it is necessary to measure weight changes continuously with respect to time at constant temperature and gas pressure, determine experimentally the dependent partial diffusion coefficients for each component, and also taking into account the gas transport occurring through the outer layer. Our test facilities allowed us to fix few of the parameters cited above. Therefore, the approach, which is introduced here, is only a very simplified qualitative model rather than a complicated mathematical treatment.

5. Conclusion

AT 900°C, UF_6 reacts with yttria at a rapid pace. The reaction mechanism was rather complex and characterised by the formation of two reaction layers: the inner layer was formed following the reaction of fluorine with substrate Y_2O_3 while the outer layer was formed by the reaction of YOF with UF_6 and UF_4. It is proposed that

[1] PB ratio volume of oxide produced/volume of metal consumed = Wd/nDw. W: molecular weight; D: density of the scale; w: molecular weight; d: density of the substrate; n: number of metal atoms in the scale molecules. D is estimated to be nearly 6.14, 4.57 g/cm^3; W: 539.82, 247.79 g; $n = 3$ and 1 for outer and inner layer, respectively. $d = 5.01$ g/cm^3.

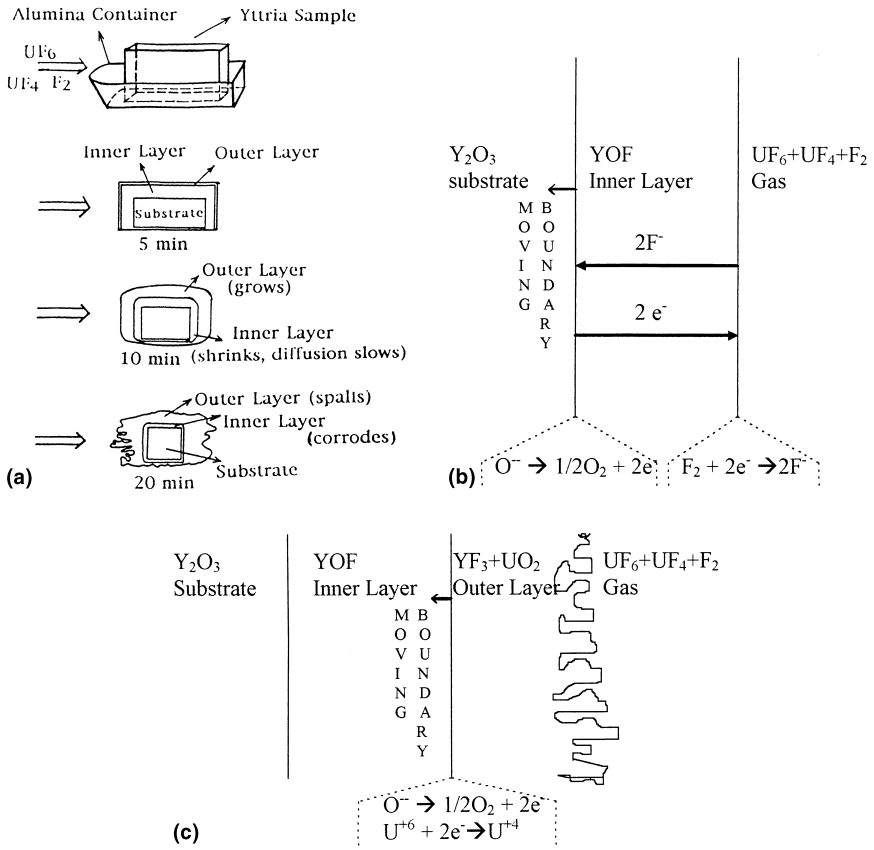

Fig. 10. (a) Schematic evolution of the corrosion. (b) Electronic exchange model after 5 min exposure. (c) Electronic exchange model after 20 min exposure.

rapid fluorine diffusion and its reaction with yttria caused the formation of the inner layer at the early stages of the exposure; however, it was found that a secondary outer layer formed later and grew by consuming the inner layer. Because of the soft and spongy character of the latter, the fluoride gases reached the interfaces rapidly and the high rate of corrosion continued even after formation of the scale. It is suggested that yttria, although a very stable oxide thermodynamically, cannot be used as a protective coating material for reactor applications in which UF_6 gas is being used as the circulating fuel at high temperatures.

Acknowledgements

This work was supported by the Strategic Defense Initiative Organisation, Innovative Science and Technology (IST) under Contract No. F33615-89-C-2919 with Wright-Patterson Air Force Base, through the Innovative Nuclear Space Power and Propulsion Institute at the University of Florida. The author would like to thank technician Tony Jones for his valuable comments and help during the experiments, TUBITAK (Turkish National Science and Technology Institute) and The University of Bath for their contribution in the preparation of this manuscript.

References

[1] C.E. Holcombe, G.W. Weber, L. Kovach, Ceram. Bull. 58 (1979) 1185.
[2] E.D. Whitney, D.J. Kim, D.S. Tucker, Nucl. Technol. 69 (1985) 154.
[3] C. Collins, master's thesis, University of Florida, Gainesville, FL 32611 (1988).
[4] S.C. Wang, S. Anghaie, D. Whitney, C. Collins, Nucl. Technol. 93 (3) (1991) 399.
[5] L. Roy, R. Furlong, L.P. Domingues, Ceram. Bull. 45 (12) (1966) 1051.
[6] J.D. Sordelet, M. Akinc, J. Am. Ceram. Soc. 71 (12) (1988) 1148.
[7] M.A. Alper, High Temperature Oxides, Academic Press, New York, 1971.
[8] P.C. Aitcin, J. Mat., JMLSA 6 (2) (1971) 282.

[9] R.T. DeHoff, Thermodynamics in Materials Science, McGraw-Hill, NewYork, 1993, pp. 326, 327.
[10] W.T. Thompson, A.D. Pelton, C.W. Bale, FACT (Facility for the Analyses of Chemical Thermodynamics) database system, Ecole Polytechnique de Montreal, Montreal, Quebec.
[11] L.M. Ferris, F.G. Baird, J. Electrochem. Soc., April (1960) p. 305.
[12] W. Bacher, K. Karlsruhe, E. Jakob, Uran, in: C. Keller, S.F. Kerntechnik, K. Karlsruhe (Eds.), Gmelin Handbuch der Anorganischen Chemie, vol. C8, Springer, Berlin, 1980.
[13] J.M. Saniger, F. Alba, S.J. Garrido, E. Avedano, Corros. Sci. 30 (8/9) (1990) 903.
[14] C. Kittel, Introduction to Solid State Physics, Wiley, New York, 1986.
[15] N. Birks, G. Meier, Introduction to High Temperature Oxidation of Metals, Edward Arnold, London, 1983, pp. 31–89.
[16] K. Hauffe, Oxidation of Metals, Plenum, New York, 1965, pp. 158–220, 276–288.
[17] R.A. Rapp, High Temperature Corrosion, NACE, Houston, 1981.
[18] G. Garnaud, The formation of a double oxide layer on pure copper, in: Oxidation of Metals, vol. 11, 1977, p. 127.
[19] D.A. Jones, Principles and Prevention of Corrosion, McMillan, New York, 1992, pp. 417 & 418.